Appl. Math. Mech. -Engl. Ed., **34**(7), 801–810 (2013)
DOI 10.1007/s10483-013-1708-9

Applied Mathematics and Mechanics (English Edition)

Separation of closely spaced modes by combining complex envelope displacement analysis with method of generating intrinsic mode functions through filtering algorithm based on wavelet packet decomposition*

Y. S. KIM[1,2], Li-qun CHEN (陈立群)[1,3,4]

(1. Shanghai Institute of Applied Mathematics and Mechanics, Shanghai 200072, P. R. China;
2. Department of Mechanics, Kim II Sung University, Pyongyang, D. P. R. Korea;
3. Department of Mechanics, College of Sciences, Shanghai University, Shanghai 200444, P. R. China;
4. Shanghai Key Laboratory of Mechanics in Energy Engineering, Shanghai University, Shanghai 200072, P. R. China)

Abstract One of the important issues in the system identification and the spectrum analysis is the frequency resolution, i.e., the capability of distinguishing between two or more closely spaced frequency components. In the modal identification by the empirical mode decomposition (EMD) method, because of the separating capability of the method, it is still a challenge to consistently and reliably identify the parameters of structures of which modes are not well separated. A new method is introduced to generate the intrinsic mode functions (IMFs) through the filtering algorithm based on the wavelet packet decomposition (GIFWPD). In this paper, it is demonstrated that the GIFWPD method alone has a good capability of separating close modes, even under the severe condition beyond the critical frequency ratio limit which makes it impossible to separate two closely spaced harmonics by the EMD method. However, the GIFWPD-only based method is impelled to use a very fine sampling frequency with consequent prohibitive computational costs. Therefore, in order to decrease the computational load by reducing the amount of samples and improve the effectiveness of separation by increasing the frequency ratio, the present paper uses a combination of the complex envelope displacement analysis (CEDA) and the GIFWPD method. For the validation, two examples from the previous works are taken to show the results obtained by the GIFWPD-only based method and by combining the CEDA with the GIFWPD method.

Key words empirical mode decomposition (EMD), wavelet packet decomposition, complex envelope displacement analysis (CEDA), closely spaced modes, modal identification

Chinese Library Classification TU311.3
2010 Mathematics Subject Classification 70J10

---

* Received Jan. 18, 2013 / Revised Feb. 19, 2013
Project supported by the State Key Program of National Natural Science of China (No. 11232009) and the Shanghai Leading Academic Discipline Project (No. S30106)
Corresponding author Li-qun CHEN, Professor, Ph. D., E-mail: lqchen@staff.shu.edu.cn

1 Introduction

One of the important issues in the system identification and the spectrum analysis is the frequency resolution, i.e., the capability of distinguishing between two or more closely spaced frequency components. In order to separate these components, it is often required to develop some special techniques or carry a large computational load. Chen and Wang[1] proposed an analytical mode decomposition theorem based on the Hilbert transform of a harmonics multiplicative time series. Feldman[2] introduced a signal decomposition formulation, called the Hilbert vibration decomposition (HVD), for vibration separation using the Hilbert transform.

In our view, more interesting techniques are those that allow separation of the closely spaced modes by the empirical mode decomposition (EMD)[3]. During the last fifteen years, with the advantage of executing a well-behaved Hilbert transform, the EMD method and the Hilbert-Huang transform (HHT) have been widely applied in the structural parameter identification and the damage detection. However, in the modal identification by the EMD, because of the separating capability of the EMD, it is still a challenge to consistently and reliably identify the parameters of structures of which modes are not well separated[1]. In the work of Rilling and Flandrin[4], through a serious mathematical consideration, a critical frequency ratio limit was obtained, which allows separation of the closest harmonics by the EMD. Yang et al.[5] proposed to use intermittence check and band-pass filter with the EMD as a preprocess tool to extract the dominant frequency components from the free vibration time histories of multi-degree-of-freedom linear systems. Zheng et al.[6] used preprocessing techniques such as the singular value decomposition (SVD) and band-pass filtering to extract modal parameters by the EMD for closely spaced modes. An interesting approach, namely, the wave group method with the EMD, was proposed by Wang[7] and combined with the orthogonal empirical mode decomposition (OEMD) by Huang et al.[8]. In Wang's study, a temporary complex time series was introduced to shift down the frequencies of its components, which could greatly increase the ratio between the higher and lower frequencies so that individual components could be separated with the EMD. However, in essence, introducing a temporary complex time series is the same procedure as the complex envelope displacement analysis (CEDA), i.e., the complex envelope displacement analysis proposed by Carcaterra and Sestieri[9].

In order to address some problems of the EMD, the authors propose a new method to generate intrinsic mode functions (IMFs) through the filtering algorithm based on the wavelet packet decomposition (GIFWPD). In this paper, it will be demonstrated that the GIFWPD method has a good capability of separating close modes, even under the severe condition beyond the critical frequency ratio limit[4,10]. However, the GIFWPD-only based method is impelled to use a very fine sampling frequency with consequent prohibitive computational costs. Therefore, in order to decrease the computational load by reducing the amount of samples and improve the effectiveness of separation by increasing the frequency ratio, we propose to use a combination of the CEDA and the GIFWPD method. For the validation, two examples from the previous works are taken to show the results by the GIFWPD-only based method and combining the CEDA with the GIFWPD method.

2 Summary of EMD method and GIFWPD method

2.1 EMD method

Any time series data $x(t)$ can be decomposed into a set of simple oscillatory functions designated as the IMFs by the EMD method as follows[3]:

$$x(t) = \sum_{k=1}^{n} c_k(t) + r_n(t). \tag{1}$$

Here, $c_k(t)\,(k = 1, 2, \cdots, n)$ are IMF components, and $r_n(t)$ is a residue term without any IMF component.

An IMF is a function that satisfies two conditions: (i) in the whole data set, the number of extrema and the number of zero-crossings must either equal or differ at most by one; and (ii) at any point, the mean value of the envelope defined by the local maxima and the envelope defined by the local minima is zero.

By the first condition, an IMF has only one extremum between two zero crossings neighboring each other, and the second condition makes an IMF symmetric with respect to zero. In results, an IMF has a unique local frequency, and different IMFs do not exhibit the same frequency at the same time.

The main procedure of the EMD method to generate the IMFs is as follows.

(i) Connect all the local maxima of the signal by a cubic spline in order to form the upper envelope. Repeat this procedure for the local minima to form the lower envelope.

(ii) The mean of upper and lower envelopes is designated as $m_1(t)$. Calculate the difference between the signal $x(t)$ and $m_1(t)$, and let $h_1(t) = x(t) - m_1(t)$. The above procedure is referred to as the sifting process. Since $h_1(t)$ still does not satisfy the requirements of the IMF, the sifting process will be performed again on $h_1(t)$ in the step (iii). If $h_1(t)$ satisfies the conditions to be an IMF, then $h_1(t)$ is the first IMF of the original signal $x(t)$. Designate it as $c_1(t) = h_1(t)$, and go to the step (iv).

(iii) If $h_1(t)$ does not satisfy the conditions for an IMF, $h_1(t)$ is treated as the original signal and repeat the steps (i)–(ii) k times until $h_{1k}(t) = h_{1(k-1)}(t) - m_{1k}(t)$ satisfies the IMF conditions. When a stopping criteria used to terminate the sifting process is smaller than a predetermined value, the first IMF $h_{1k}(t)$ is obtained. Then, it is designated as $c_1(t) = h_{1k}(t)$, the first IMF of $x(t)$.

(iv) Separate $c_1(t)$ from $x(t)$ to get $r_1(t) = x(t) - c_1(t)$. Here, $r_1(t)$ is treated as the original data, and by repeating the above steps (i)–(iii), the second IMF $c_2(t)$ can be obtained.

(v) Repeat the steps (i)–(iv) n times to get n IMFs. If $r_n(t)$ does not contain any component satisfied with the IMF conditions, terminate the whole procedure. Here, $r_n(t)$ is the residue term, which usually is a constant, a monotonic slope, or a function with only one extremum.

Performing the above procedure, we can decompose $x(t)$ into n IMFs and one residue term yielding the equation (1). The residue term $r_n(t)$ represents the tendency of the signal $x(t)$.

Although the EMD method has a great ability to extract the properties of nonlinear and non-stationary signals, it has still a number of problems that need further attention. Especially, the EMD-only based method is not so effective to decompose closely spaced frequency components.

2.2 GIFWPD method

In the GIFWPD method, the wavelet packet analysis is used to decompose the inspected original signal into many narrow-banded sub-signals for the later filtering processing. The wavelet packet analysis is a generalization of wavelet decomposition. In the wavelet packet decomposition procedure, a successive detail coefficient vector is also decomposed into two parts using the same approach as in the approximation vector splitting. Each sub-signal has the same frequency bandwidth. This offers the richest analysis of a signal.

At an enough decomposition level, each reconstructed terminal node of the wavelet packet decomposition tree becomes a narrow-band filtered sub-signal. The reconstructed terminal nodes corresponding to a relatively higher frequency region will satisfy the IMF conditions well. If each of the frequency bands of these terminal nodes is narrow enough, the sum of these two or more reconstructed nodes will also be narrow-banded sub-signal and should still satisfy the IMF conditions. That is, it can be said that the sum of a certain number of reconstructed nodes corresponding to a relatively higher frequency region will also generate an IMF. According to the ways of summing up the reconstructed nodes, a variety of decomposition into IMFs can be obtained. An approach of summing up the terminal nodes to guarantee the uniqueness of the decomposition into IMFs can be established by making the frequency band of each IMF as wide as possible but non-overlapped with each other.

The below describes how to realize the whole procedure of the approach.

(i) Decompose the signal $x(t)$ into wavelet packet decomposition tree. If necessary, find the best tree with the criterion of Shannon entropy. By rearranging the naturally ordered terminal nodes in order of decreasing frequency, get the inversely reordered terminal nodes $T_j\,(j = 1, 2, \cdots, N)$ with T_1 corresponding to the highest frequency band and T_N corresponding to the lowest frequency band. Reconstruct $T_j\,(j = 1, 2, \cdots, N)$ to produce $u_j(t)\,(j = 1, 2, \cdots, N)$ in the time domain. Initialize the parameter i for counting IMFs as $i = 1$ and the index number s_i for the reference node as $s_i = 1$.

(ii) Set the parameter p to which the sum of the terminal nodes starting with the reference node is computed as $p = N$.

(iii) Check if $h(t) = \sum\limits_{j=s_i}^{p} u_j(t)$ satisfies the IMF conditions or not. If $h(t)$ does not satisfy the IMF conditions, then set $p := p - 1$ and repeat the step (iii) until $h(t)$ satisfies the IMF conditions. If it is the first iteration, as discussed above, for a certain p, there must be at least one IMF. If it is not the first iteration, having already passed the step (v) guarantees that, for a certain p, there must be an IMF.

(iv) For a certain p, if $h(t)$ satisfies the IMF conditions, it is designated as $c_i(t) = h(t)$, the ith IMF of the signal $x(t)$. Then, calculate $r(t) = x(t) - \sum\limits_{k=1}^{i} c_k(t)$.

(v) If $r(t)$ is still an oscillating signal, set $i := i + 1$, $s_i := p + 1$ and return to the step (ii). If $r(t)$ is a non-oscillating signal, terminate the loop. $r(t)$ is the residue term.

Performing the above proposed algorithm, we can get the IMF decomposition formula of the signal $x(t)$ as

$$\begin{aligned} x(t) &= \sum_{j=s_1}^{s_2-1} u_j(t) + \sum_{j=s_2}^{s_3-1} u_j(t) + \cdots + \sum_{j=s_{n-1}}^{s_n-1} u_j(t) + \sum_{j=s_n}^{N} u_j(t) \\ &= \sum_{i=1}^{n} \sum_{j=s_i}^{s_{i+1}-1} u_j(t) + r(t) \\ &= \sum_{i=1}^{n} c_i(t) + r(t). \end{aligned} \tag{2}$$

3 Separating two closely spaced harmonics by GIFWPD-only based method

According to Feldman[10], the ability of the EMD to separate two harmonics depends upon the frequency ratio and the amplitude ratio of the two components. Its theoretical limit that does not depend on the amplitude relations between the harmonics is $\omega_2/\omega_1 \leqslant 1.5$. This theoretical limit value completely coincides with the experimental critical frequency ratio $\omega_1/\omega_2 \approx 0.67$, that is, $\omega_2/\omega_1 \approx 1.5$ found in the work of Rilling and Flandrin[4]. Within this value, it is impossible to separate two components by the EMD-only based method, no matter what the amplitude ratio is.

In this section, we shall revisit an example presented originally in [7] to show that the GIFWPD method alone has a good capability of separating close modes, even under the severe condition beyond the critical frequency ratio limit, provided that the computational costs are permitted.

Consider a pair of closely spaced cosine waves given by

$$x(t) = \cos\Big(\frac{2}{30}\pi t\Big) + \cos\Big(\frac{2}{32}\pi t + \frac{\pi}{6}\Big). \tag{3}$$

The frequencies of these two harmonics are approximately 0.0333 Hz and 0.0313 Hz, and the frequency ratio is approximately 1.067. This signal shows the characteristic beat phenomena (see Fig. 1).

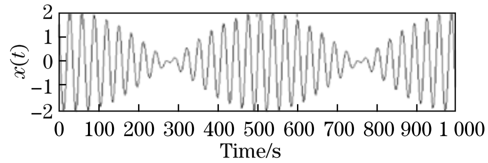

Fig. 1 Wave profile represented by Eq. (3)

In order to separate these two components by the GIFWPD-only based method, a very fine sampling frequency 200 Hz is needed. At the first sight, this sampling frequency might appear as ordinary, but it is a considerably large value in contrast to the low frequencies of the two harmonics.

Figure 2 shows the separation results, i.e., the first mode $c_1(t)$ and the second mode $c_2(t)$ decomposed by the GIFWPD method in comparison with theoretical modes. The results agree well with the theoretical modes except for the beginning and end of the signals which have slight distortion. However, for a relatively low sampling frequency 1 Hz, the GIFWPD method failed to separate these two modes although a correct representation of the two harmonics can be obtained enough with this sampling frequency.

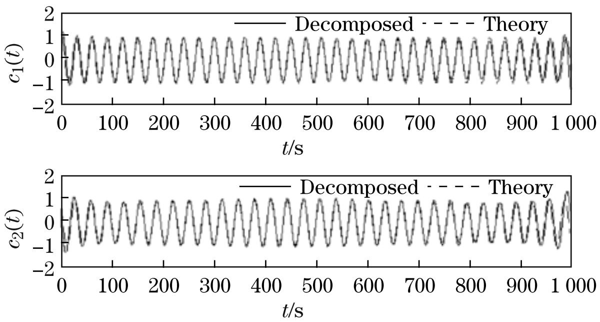

Fig. 2 Two modes decomposed by GIFWPD method and theoretical modes

Although the successful separation is performed by a very fine sampling frequency, the results show that the GIFWPD method alone has a good capability of separating close modes provided that computational costs are permitted. In order to decrease the computational load by reducing the amount of samples and improve the effectiveness of separation by increasing the frequency ratio, we propose to use a combination of the CEDA and the GIFWPD method.

4 Separation of closely spaced modes by combining CEDA with GIFWPD method

4.1 Theoretical background

The CEDA was originally proposed by Carcaterra and Sestieri[9], aiming at obtaining some desirable properties rather than the actual solution itself of a system by means of the envelope analysis which can decrease the computational load for the structure-acoustic coupled problems.

Suppose that the two closely spaced modes are expressed as

$$\begin{cases} x_1(t) = A_1(t)\cos\Phi_1(t), \\ x_2(t) = A_2(t)\cos\Phi_2(t). \end{cases} \tag{4}$$

Then, the summed signal $x(t) = x_1(t) + x_2(t)$ is a narrow-banded signal with a frequency band around a mean frequency f_0 which is equal to a mean value of time derivatives of two phase angles, $\Phi_1(t)$ and $\Phi_2(t)$. That is, if $\mathrm{d}\Phi_1(t)/\mathrm{d}t$ and $\mathrm{d}\Phi_2(t)/\mathrm{d}t$ are approximately equal to f_1 and f_2, respectively, they are bands limited around the mean frequency f_0, i.e., $f_1, f_2 \in [f_0 - f_\Delta, f_0 + f_\Delta]$ (f_0 is the mean frequency, and f_Δ is the tiny sphere of f_0).

For a phase delay $v(t) = 2\pi\,(f_0 - f_\Delta)t$, the complex envelope displacement of $x(t)$ is defined as[9]

$$\breve{x}(t) = x_{\mathrm{a}}(t)\mathrm{e}^{-\mathrm{i}v(t)}. \tag{5}$$

Here, $x_{\mathrm{a}}(t)$ is the analytical signal of $x(t)$ defined as

$$x_{\mathrm{a}}(t) = x(t) + \mathrm{i}\widetilde{x}(t), \tag{6}$$

where $\widetilde{x}(t)$, the Hilbert transform of $x(t)$, is

$$\widetilde{x}(t) = \frac{1}{\pi}\int_{-\infty}^{\infty}\frac{x(\tau)}{t-\tau}\mathrm{d}\tau. \tag{7}$$

Assume that $A_1(t)$ and $A_2(t)$ are the frequency signals relatively lower than $\cos\Phi_1(t)$ and $\cos\Phi_2(t)$, and their spectra are not overlapped each other. The analytical signals of $x_1(t)$ and $x_2(t)$ can be expressed as

$$\begin{cases} x_{1\mathrm{a}}(t) = x_1(t) + \mathrm{i}\widetilde{x}_1(t) \\ \qquad\quad\ = A_1(t)\cos\Phi_1(t) + \mathrm{i}A_1(t)\sin\Phi_1(t) \\ \qquad\quad\ = A_1(t)\mathrm{e}^{\mathrm{i}\Phi_1(t)}, \\ x_{2\mathrm{a}}(t) = x_2(t) + \mathrm{i}\widetilde{x}_2(t) \\ \qquad\quad\ = A_2(t)\cos\Phi_2(t) + \mathrm{i}A_2(t)\sin\Phi_2(t) \\ \qquad\quad\ = A_2(t)\mathrm{e}^{\mathrm{i}\Phi_2(t)}. \end{cases} \tag{8}$$

Using the linearity of the Hilbert transform, $x_{\mathrm{a}}(t)$ can be written as

$$x_{\mathrm{a}}(t) = x_{1\mathrm{a}}(t) + x_{2\mathrm{a}}(t). \tag{9}$$

Substituting Eqs. (9) and (8) into Eq. (5) yields

$$\begin{aligned} \breve{x}(t) &= (A_1(t)\mathrm{e}^{\mathrm{i}\Phi_1(t)} + A_2(t)\mathrm{e}^{\mathrm{i}\Phi_2(t)})\mathrm{e}^{-\mathrm{i}v(t)} \\ &= A_1(t)\cos(\Phi_1(t) - v(t)) + A_2(t)\cos(\Phi_2(t) - v(t)) \\ &\quad + \mathrm{i}(A_1(t)\sin(\Phi_1(t) - v(t)) + A_2(t)\sin(\Phi_2(t) - v(t))). \end{aligned} \tag{10}$$

Its real part is given by

$$\begin{aligned} \breve{x}_{\mathrm{R}}(t) &= \mathrm{Re}(\breve{x}(t)) \\ &= A_1(t)\cos(\Phi_1(t) - v(t)) + A_2(t)\cos(\Phi_2(t) - v(t)). \end{aligned} \tag{11}$$

From Eq. (11), it is found that $\breve{x}_{\mathrm{R}}(t)$ is a frequency-shifted signal consisting of two signal components that are low frequency signals with the phase delay $v(t)$ for two original mode functions, $x_1(t)$ and $x_2(t)$. It is also found that the difference between the two low frequencies is still the same as the original frequency difference $\dot{\Phi}_1(t) - \dot{\Phi}_2(t)$. This indicates that the frequency ratio of the two components can be increased significantly. Therefore, the separation of two components by the GIFWPD method can be done with ease. For the two low frequency signal components, down-sampling can be applied to reduce the amount of samples while keeping the correct representation of the signal and the original frequency difference.

Thus, by performing down-sampling on $\overleftarrow{x}_{\mathrm{R}}(t)$ and then applying the GIFWPD method to the re-sampled signal, the two low frequency-shifted components can be easily decomposed, i.e.,

$$\begin{cases} \overleftarrow{x}_1(t) = A_1(t)\cos(\Phi_1(t) - v(t)), \\ \overleftarrow{x}_2(t) = A_2(t)\cos(\Phi_2(t) - v(t)). \end{cases} \tag{12}$$

Then, by performing up-sampling on the separated $\overleftarrow{x}_1(t)$ and $\overleftarrow{x}_2(t)$ to restore their original lengths and the multiplication with $\mathrm{e}^{\mathrm{i}v(t)}$ on their analytical signals, $\overleftarrow{x}_{1\mathrm{a}}(t)$ and $\overleftarrow{x}_{2\mathrm{a}}(t)$ to restore their original frequencies, we can obtain

$$\begin{cases} \vec{x}_{1\mathrm{a}}(t) = \overleftarrow{x}_{1\mathrm{a}}(t)\mathrm{e}^{\mathrm{i}v(t)} \\ \qquad\quad = A_1(t)\mathrm{e}^{\mathrm{i}(\Phi_1(t)-v(t))}\mathrm{e}^{\mathrm{i}v(t)} \\ \qquad\quad = A_1(t)\mathrm{e}^{\mathrm{i}\Phi_1(t)}, \\ \vec{x}_{2\mathrm{a}}(t) = \overleftarrow{x}_{2\mathrm{a}}(t)\mathrm{e}^{\mathrm{i}v(t)} \\ \qquad\quad = A_2(t)\mathrm{e}^{\mathrm{i}(\Phi_2(t)-v(t))}\mathrm{e}^{\mathrm{i}v(t)} \\ \qquad\quad = A_2(t)\mathrm{e}^{\mathrm{i}\Phi_2(t)}. \end{cases} \tag{13}$$

From Eq. (13), it is obvious that the original two modes can be obtained by

$$\begin{cases} x_1(t) = \mathrm{Re}(\vec{x}_{1a}(t)), \\ x_2(t) = \mathrm{Re}(\vec{x}_{2a}(t)). \end{cases} \tag{14}$$

Here, if $x_1(t)$ and $x_2(t)$ are natural modes originated from a linear vibration system, then their instantaneous amplitudes and the instantaneous phase angles can be represented as follows[5]:

$$\begin{cases} A_k(t) = A_k\mathrm{e}^{-\zeta_k\omega_{\mathrm{n}k}t}, \\ \Phi_k(t) = \omega_{\mathrm{d}k}t + \theta_k, \end{cases} \tag{15}$$

where A_k is the modal amplitude, ζ_k is the modal damping ratio, $\omega_{\mathrm{n}k}$ is the undamped natural angular frequency, $\omega_{\mathrm{d}k}$ is the damped natural angular frequency, and θ_k is the initial phase angle for $k = 1, 2$. From Eq. (15), the following can be obtained:

$$\begin{cases} \ln A_k(t) = -\zeta_k\omega_{\mathrm{n}k}t + \ln A_{ijk}, \\ \omega_{\mathrm{d}k} = \dfrac{\mathrm{d}\Phi_k(t)}{\mathrm{d}t}. \end{cases} \tag{16}$$

From Eq. (16), it is found that $\omega_{\mathrm{d}k}$ is the same as the slope of the phase angle time history $\Phi_k(t)$, and $-\zeta_k\omega_{\mathrm{n}k}$ is the slope of the straight line of the decaying amplitude $\ln A_k(t)$ plotted in a logarithmic scale. Therefore, we can estimate ζ_k, $\omega_{\mathrm{n}k}$, θ_k, and A_k using the linear least-square fit for $\ln A_k(t)$ and $\Phi_k(t)$.

4.2 Numerical examples for system identification with closely spaced modes

For validation of the proposed method, we shall revisit an example presented originally by Chen and Wang[1]. Consider a linear vibration system of three-degree-of-freedom as shown in Fig. 3. The system has three masses of $m_1 = m_2 = m_3 = 1\,000$ kg, four springs with the stiffness of $k_1 = k_4 = 40$ kN/m and $k_2 = k_3 = 15$ kN/m, and four dashpots with the damping coefficients of $c_1 = c_4 = 120$ N·s/m and $c_2 = c_3 = 45$ N·s/m. The system has three natural frequencies of $f_1 = 0.673$ Hz, $f_2 = 1.180$ Hz, and $f_3 = 1.304$ Hz. The 2nd and 3rd natural frequencies are closely spaced, and their frequency ratio is approximately 1.105. An initial velocity of 0.1 m/s is applied on the mass m_3 at $t = 0$ s. The acceleration time history $x(t)$ at the mass m_1 is calculated with Simulink (MATLAB) and used for system identification. A time step of 0.000 15 s is used in the numerical integrations. Figure 4 shows the acceleration response at the mass m_1 and its power spectrum $X(f)$.

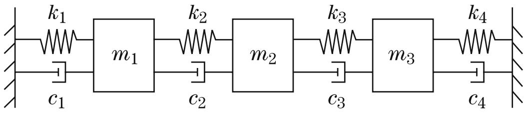

Fig. 3 Linear vibration system of three-degree-of-freedom

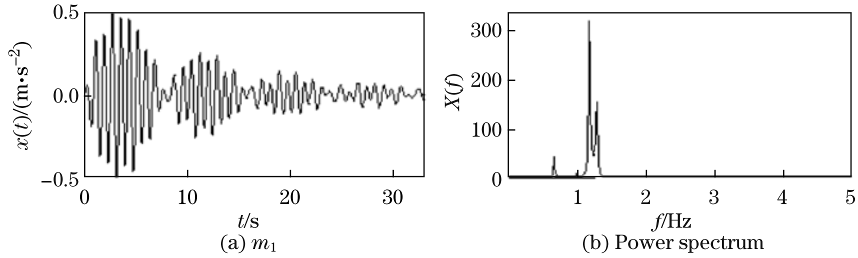

Fig. 4 Acceleration time history at mass m_1 and its power spectrum

The CEDA with a phase shifting of $v(t) = 2\pi \times 0.55t$ is performed on the acceleration response, and the down-sampling is done with the re-sampling rate of 0.015 s. By applying the GIFWPD method to the real part of the down-sampled signal, three low frequency components $\overleftarrow{x}_1(t)$, $\overleftarrow{x}_2(t)$, and $\overleftarrow{x}_3(t)$ are decomposed. After that, by performing up-sampling on the separated low frequency components to restore their original lengths and multiplying with $e^{iv(t)}$ on their analytical signals to restore their original frequencies, three natural modes $x_1(t)$, $x_2(t)$, and $x_3(t)$ of the system are obtained as shown in Fig. 5.

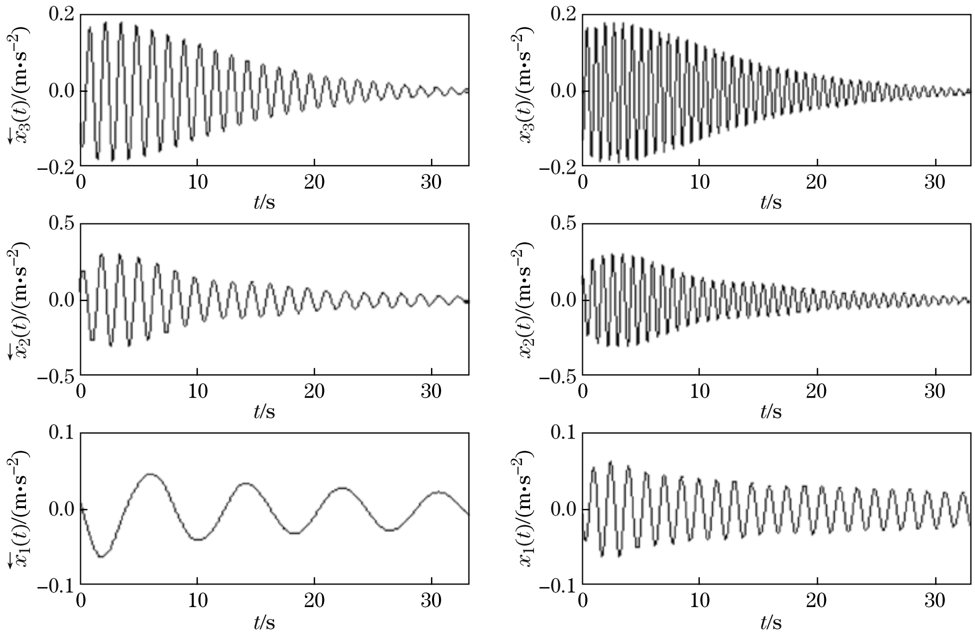

Fig. 5 Frequency-shifted modes (left) and natural modes (right) separated by GIFWPD method

Figure 6 presents the logarithmic instantaneous scaled amplitudes $\ln A_1(t)$, $\ln A_2(t)$, and $\ln A_3(t)$ and the instantaneous phase angles $\Phi_1(t)$, $\Phi_2(t)$, and $\Phi_3(t)$ of each mode, from which the natural frequencies and damping ratios are identified according to Eqs. (15) and (16). The result of identification is given in Table 1.

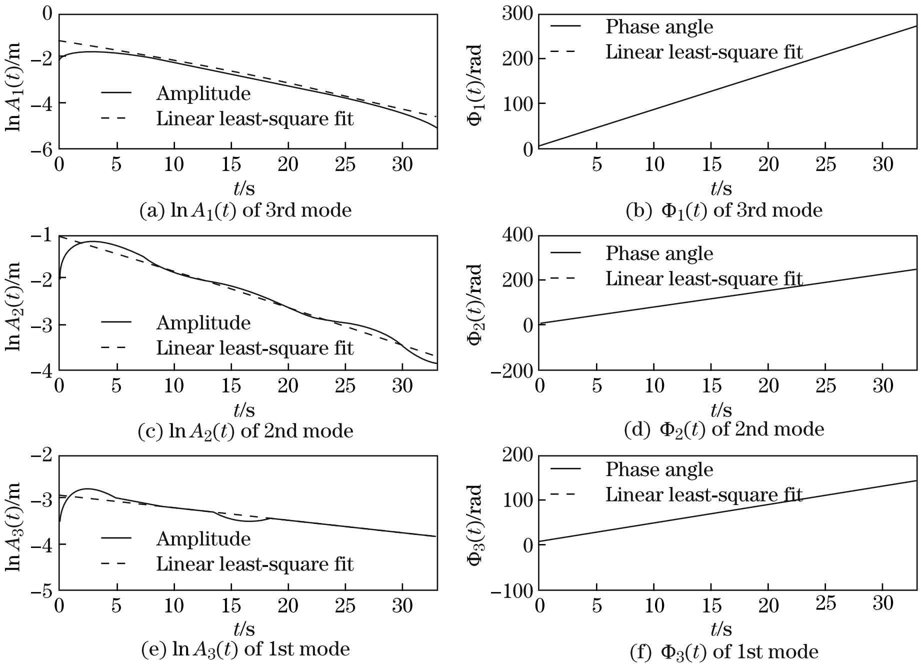

Fig. 6 Logarithmic scaled amplitude and its linear least-square fit (left) and phase angle and its linear least-square fit (right)

Table 1 Identified natural frequencies and damping ratios

Mode	Natural frequency/Hz		Damping ratio/%	
	Theory	Identification	Theory	Identification
1	0.673	0.673	0.63	0.68
2	1.180	1.181	1.11	1.10
3	1.304	1.302	1.23	1.25

5 Conclusions

The numerical example in Section 3 shows that the GIFWPD method alone has a good capability of separating close modes, even under the severe condition beyond the critical frequency ratio limit. However, the GIFWPD-only based method is impelled to use a very fine sampling frequency with heavy computational cost. In order to decrease the computational load by reducing the amount of samples and improve the effectiveness of separation by increasing the frequency ratio, a combination of the CEDA and the GIFWPD method is proposed in this paper.

The CEDA naturally has more effectiveness for problems that concern very high frequencies. However, the natural frequencies exampled in subsection 4.2 are in low frequency band rather than high frequency band, which is an adverse condition to the proposed method. Furthermore, the numerical simulation in subsection 4.2 is performed without a high-pass filtering process which is usual with many other decomposition methods. Nevertheless, the result of identification is good enough to indicate that the proposed method is an effective approach in separating closely spaced frequency components. However, a careful consideration is needed for the selection of the phase delay of the complex envelope displacement.

References

[1] Chen, G. and Wang, Z. C. A signal decomposition theorem with Hilbert transform and its application to narrowband time series with closely spaced frequency components. *Mechanical Systems and Signal Processing*, **28**, 258–279 (2012)

[2] Feldman, M. Time-varying vibration decomposition and analysis based on the Hilbert transform. *Journal of Sound and Vibration*, **295**, 518–530 (2006)

[3] Huang, N. E., Shen, Z., Long, S. R., Wu, M. C., Shih, H. H., Zheng, Q. N., Yen, N. C., Tung, C. C., and Liu, H. H. The empirical mode decomposition and the Hilbert spectrum for non-linear and non-stationary time series analysis. *Proceedings of the Royal Society London A*, **454**, 903–995 (1998)

[4] Rilling, G. and Flandrin, P. One or two frequencies? The empirical mode decomposition answers. *IEEE Transactions on Signal Processing*, **56**(1), 85–95 (2008)

[5] Yang, J. N., Lei, Y., Pan, S. W., and Huang, N. System identification of linear structures based on Hilbert-Huang spectral analysis, part 1: normal modes. *Earthquake Engineering and Structural Dynamics*, **32**, 1443–1467 (2003)

[6] Zheng, M., Shen, F., Dou, Y. P., and Yan, X. Y. Modal identification based on Hilbert-Huang transform of structural response with SVD preprocessing. *Acta Mechanica Sinica*, **25**, 883–888 (2009)

[7] Wang, W. Decomposition of wave groups with EMD method. *The Hilbert-Huang Transform in Engineering* (eds. Huang, N. and Attoh-Okine, N.), CRC Press, Boca Raton, 267–280 (2005)

[8] Huang, T. L., Qiu, F. Q., and Lou, M. L. Application of an improved HHT method for modal parameters identification of structures with closely spaced modes (in Chinese). *Journal of Central South University* (*Science and Technology*), **42**(7), 2054–2062 (2011)

[9] Carcaterra, A. and Sestieri, A. Complex envelope displacement analysis: a quasi-static approach to vibrations. *Journal of Sound and Vibration*, **201**, 205–233 (1997)

[10] Feldman, M. Analytical basics of the EMD: two harmonics decomposition. *Mechanical Systems and Signal Processing*, **23**, 2059–2071 (2009)